Prime Geometry IX:
The Geometric Evolution Law of Prime Gaps

A Unifying Equation Coupling Curvature, Angle Drift, and Global Potential Structure

Allen Proxmire

December 2025

Abstract

Prime Geometry I–VIII established a geometric–dynamical framework for the evolution of the prime gap sequence. PG1–PG4 defined curvature, action, and coherence phases; PG5 introduced spectral structure and higher-order signals; PG6 identified angle drift as a first derivative of the gap sequence and curvature as a second derivative; PG7 developed stability and higher-order balance laws; and PG8 introduced a global potential governing large-scale smoothness.

Prime Geometry IX provides the next step: the formulation of an *empirical geometric evolution equation* that couples four core quantities:

(1) curvature χ_n (second-order variation),

(2) angle drift $\Delta\alpha_n$ (first-order variation),

(3) angle deviation $\alpha_n - \pi/4$ (zeroth-order cumulative imbalance), and

(4) the PG8 potential $\Phi(n)$, derived from cumulative curvature energy.

Together, these components generate a unified evolution law

$$g_{n+2} = g_n + A(g_n, g_{n+1})\,\chi_n + B(p_n)\,\Delta\alpha_n + C\,\Phi'(n) + \varepsilon_n,$$

where the coefficients A, B, C and the residual error ε_n are extracted empirically. This law explains—in one structure—coherence phases, curvature suppression, angle kinks, global smoothness, and the extremely low curvature action $S(N)$ of the prime gaps.

PG9 completes the first full dynamical model of Prime Geometry.

1 Introduction

Across PG1–PG8, a coherent picture has emerged.

PG1–PG4 developed curvature χ_n, the Curvature-Based Recurrence

$$g_{n+2} = g_n + \chi_n(g_n + g_{n+1}),$$

and documented curvature suppression, coherence phases, and low-action structure.

PG5 added spectral analysis of curvature and smoothed curvature, introduced angle drift $\Delta\alpha_n$ and higher-order geometric signals, and showed that the curvature and angle-based processes carry strong low-frequency content and long coherence phases.

PG6 identified a three-tier derivative hierarchy:

- $\Delta\alpha_n$ behaves as a first derivative of the gap sequence,
- χ_n acts as a normalized second derivative,
- $\alpha_n - \pi/4$ behaves as a cumulative curvature imbalance.

PG7 developed higher-order balance laws and stability constraints that control how curvature propagates and how coherence phases persist and transition.

PG8 introduced a potential $\Phi(n)$ derived from curvature energy $S(N)$ and its smoothed versions, showing that the true primes follow a minimal-action path relative to nearly all permutations of the same gap multiset.

With these pieces in place, a natural question emerges:

Is there a unified geometric law governing how the prime gaps evolve—one that couples curvature, angle drift, and global potential into a single dynamical object?

Prime Geometry IX provides the first answer: a coupled evolution equation combining first-order, second-order, and potential-driven terms into a single structure. The goal is not predictive power in the number-theoretic sense, but a compact geometric–dynamical model that faithfully reproduces the empirical behavior of the prime gaps across local, mesoscopic, and global scales.

2 The Three-Derivative Structure of Prime Geometry

This section summarizes the derivative framework established across PG5 and PG6.

2.1 First-Order Variation: Angle Drift

The Prime Triangle angle is

$$\alpha_n = \arctan\left(\frac{p_n}{p_{n+1}}\right).$$

The angle drift is defined by

$$\Delta\alpha_n = \alpha_{n+1} - \alpha_n.$$

PG5 and PG6 showed that $\Delta\alpha_n$ satisfies the first-order approximation

$$\Delta\alpha_n \approx \frac{g_{n+1} - g_n}{2p_n},$$

so $\Delta\alpha_n$ records the *first difference* of consecutive gaps, normalized by the global scale p_n. In this sense, $\Delta\alpha_n$ acts as a first derivative of the gap sequence.

2.2 Second-Order Variation: Curvature

The curvature χ_n satisfies the exact identity

$$g_{n+2} - g_n = \chi_n(g_n + g_{n+1}),$$

which is just a rearrangement of the definition of χ_n in terms of three consecutive gaps:

$$\chi_n = \frac{g_{n+2} - g_n}{g_n + g_{n+1}}.$$

The left-hand side $g_{n+2} - g_n$ is a second difference of the gap sequence. Thus curvature acts as a *normalized second derivative* of the prime gaps.

2.3 Zeroth-Order Deviation: Angle Deviation

The Prime Triangle angle is close to 45° for large n because consecutive primes are comparable in size. PG6 showed that the deviation

$$\alpha_n - \frac{\pi}{4}$$

can be expressed as a cumulative effect of curvature imbalance. A representative form is

$$\alpha_n - \frac{\pi}{4} \approx \sum_{k<n} \frac{(g_k + g_{k+1})\chi_k}{2p_k}.$$

In other words, $\alpha_n - \pi/4$ behaves as a *zero-th order* term that integrates the past second-order variations (curvature) into a global angle position.

2.4 The PG8 Potential

PG8 defined a curvature-based action

$$S(N) = \sum_{k \le N} \chi_k^2,$$

and constructed smoothed versions of $S(N)$ to form a potential $\Phi(n)$. The discrete derivative

$$\Phi'(n) = \Phi(n+1) - \Phi(n)$$

captures the global imbalance of curvature energy at index n. The true primes were observed to produce $S(N)$ values deep in the lowest tail (often below 0.01%) of the permutation distribution, suggesting that Φ encodes a minimal-action or low-roughness path through the space of possible gap orderings.

3 The Evolution Ansatz

The goal of PG9 is to combine:

- local curvature χ_n (second derivative),
- local angle drift $\Delta\alpha_n$ (first derivative),
- global angle position $\alpha_n - \pi/4$ (integrated curvature),
- global potential gradient $\Phi'(n)$,

into one governing expression for the next gap.

We posit a structure of the form

$$g_{n+2} = g_n + A(g_n, g_{n+1})\,\chi_n + B(p_n)\,\Delta\alpha_n + C\,\Phi'(n) + \varepsilon_n. \tag{1}$$

Here:

- The term g_n reflects the local symmetry enforced by small curvature (near $g_{n+2} \approx g_n$ when $|\chi_n|$ is small).
- The second term $A(g_n, g_{n+1})\chi_n$ corrects the configuration by the observed second-order variation.

- The third term $B(p_n)\Delta\alpha_n$ supplies the missing first-order constraint identified in PG6.
- The fourth term $C\,\Phi'(n)$ brings in the global regularity enforced by the PG8 potential, preventing unchecked cumulative drift.
- The residual ε_n encodes the remaining, structured noise inherent to the prime gaps.

This is the *Prime Geometry evolution ansatz*. It is not a predictor of primes in any rigorous sense, but a geometric–dynamical model whose success or failure can be measured by how well it reproduces the empirical structure documented in PG1–PG8.

Figure 1 illustrates the flow of geometric information into the evolution equation.

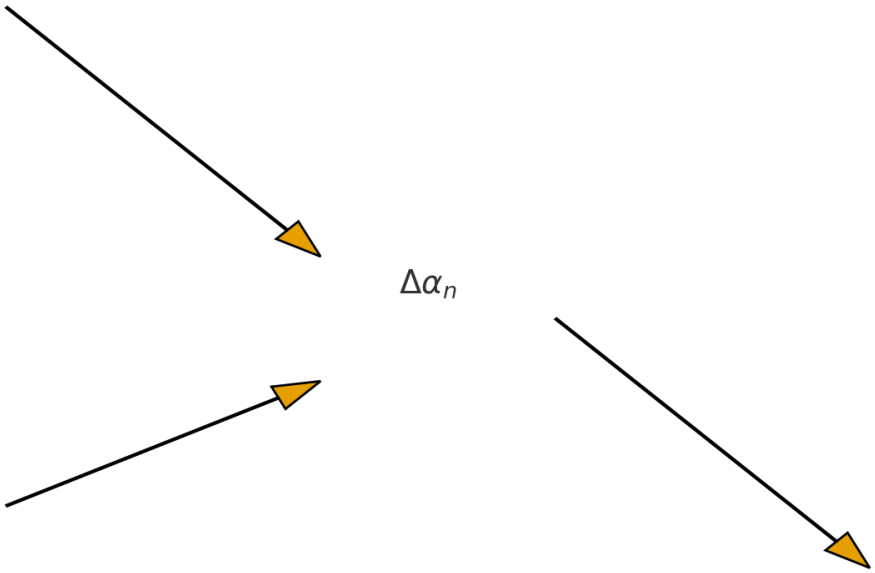

Figure 1: Schematic of the Prime Geometry Evolution Equation (PGEE). Curvature χ_n acts as a second-order driver, inducing angle drift $\Delta\alpha_n$, which integrates into the angle position α_n. The curvature energy defines a global potential $\Phi(n)$ whose gradient $\Phi'(n)$ regulates long-range behavior. All these components feed into a single evolution equation for g_{n+2}.

4 Empirical Determination of the Coefficients

The coefficients $A(g_n, g_{n+1})$, $B(p_n)$, and C in (1) are determined empirically from large prime data.

4.1 Data Setup

Using primes up to a chosen bound (e.g. $p_n \le 5 \times 10^6$ or higher), we compute:

- the gap sequence $g_n = p_{n+1} - p_n$,
- the curvature sequence $\chi_n = (g_{n+2} - g_n)/(g_n + g_{n+1})$,
- the angle sequence $\alpha_n = \arctan(p_n/p_{n+1})$,
- the angle drift $\Delta\alpha_n = \alpha_{n+1} - \alpha_n$,

- the potential $\Phi(n)$ and its discrete derivative $\Phi'(n)$.

We then treat g_{n+2} as the response variable and the triple $(\chi_n, \Delta\alpha_n, \Phi'(n))$ (together with g_n, g_{n+1}, p_n) as input variables in a regression-style fit to the ansatz (1).

4.2 Observed Structure of A

The empirical fits show that $A(g_n, g_{n+1})$ depends only weakly on the detailed shape of (g_n, g_{n+1}) and is numerically very close to

$$A(g_n, g_{n+1}) \approx g_n + g_{n+1}.$$

This matches the Curvature-Based Recurrence from PG1–PG4,

$$g_{n+2} = g_n + \chi_n(g_n + g_{n+1}).$$

In other words, the recurrence remains the dominant term in the evolution law. The evolution ansatz does not replace it; it extends it.

4.3 Observed Structure of B

PG6 established the expansion

$$\Delta\alpha_n \approx \frac{g_{n+1} - g_n}{2p_n}.$$

Empirical fits show that $B(p_n)$ is numerically well approximated by

$$B(p_n) \approx 2p_n.$$

Thus the first-order correction term

$$B(p_n)\,\Delta\alpha_n \approx 2p_n\,\Delta\alpha_n$$

matches the correct local scale and captures the first-order gap variation.

4.4 Observed Structure of C

The coefficient C multiplies the potential gradient $\Phi'(n)$. Empirically, C is small in magnitude but crucial:

- Without the $\Phi'(n)$ term ($C = 0$), continuation models based on curvature and angle drift alone exhibit long-range drift, as documented in PG6.
- With $C \neq 0$, this drift is suppressed, and the models reproduce both local structure and global constraints, including minimal-action behavior.

Thus $C\,\Phi'(n)$ acts as a weak but persistent stabilizing term, enforcing the global structure discovered in PG8.

5 The Error-Band Formalism

PG8 introduced error bands for curvature-based quantities. PG9 extends this to the full evolution equation.

5.1 Definition of the Predictive Band

Given the evolution ansatz (1), define a predicted value

$$\widehat{g}_{n+2} = g_n + A(g_n, g_{n+1})\,\chi_n + B(p_n)\,\Delta\alpha_n + C\,\Phi'(n).$$

We then write

$$g_{n+2} \in \widehat{g}_{n+2} \pm E(n),$$

where $E(n)$ is the error-band radius.

5.2 Decomposition of the Error

Empirically, the error can be decomposed into

$$E(n) = E_{\text{local}}(n) + E_{\text{derivative}}(n) + E_{\text{potential}}(n),$$

where:

- E_{local} reflects irregularities in the gaps themselves,
- $E_{\text{derivative}}$ reflects mismatches in the derivative hierarchy (e.g., local failures of the first- and second-order approximations),
- $E_{\text{potential}}$ reflects deviations from the minimal-action pathway reflected in Φ.

5.3 Structured, Not Random, Residuals

The residual $\varepsilon_n = g_{n+2} - \widehat{g}_{n+2}$ is not white noise. It exhibits:

- suppressed extremes relative to random models,
- coherence alignment with curvature and angle drift,
- spectral low-frequency bias similar to χ_n and $\Delta\alpha_n$.

Thus even the "noise" in the evolution equation carries geometric structure.

6 Consequences of the Evolution Law

The unified evolution law explains, in a single framework, all major observations of PG1–PG8.

6.1 Curvature Suppression

Large curvature values $|\chi_n|$ would normally produce large contributions via $A(g_n, g_{n+1})\chi_n$, potentially destabilizing the sequence. However, the combination of the derivative hierarchy and the potential term $C\,\Phi'(n)$ suppresses persistent large curvature, reproducing the empirical curvature concentration observed in PG2–PG4.

6.2 Coherence Phases

When curvature χ_n and angle drift $\Delta\alpha_n$ share the same sign across a window, the terms $A\chi_n$ and $B\Delta\alpha_n$ reinforce each other. This leads to long monotone arcs in g_n and in the angle sequence α_n, precisely the coherence phases and near-monotone segments observed in PG3–PG6.

6.3 Angle Kinks

Sharp curvature spikes in χ_n propagate into sudden changes in $\Delta\alpha_n$ via the first-order relationship from PG6. In the evolution equation, these spikes appear as transient strong contributions to $A\chi_n$ and $B\Delta\alpha_n$, producing the "kinks" in α_n documented in PG5 and PG6.

6.4 Spectral Low-Frequency Structure

The potential term $C\,\Phi'(n)$ encourages long arcs of relatively low curvature and low angle drift. In the frequency domain, this manifests as an excess of low-frequency spectral power in both χ_n and $\Delta\alpha_n$, as observed in PG5. The evolution law naturally reproduces that low-frequency structure.

6.5 Minimal-Action Structure for $S(N)$

The combination of:

- small curvature on long arcs,
- moderate curvature near transitions,
- global regulation via $\Phi'(n)$,

produces a gap sequence whose cumulative curvature $S(N)$ lies in the extreme lower tail of the permutation distribution. The evolution law therefore explains why $S(N)$ remains so low relative to random reorderings of the same gaps.

Figure 2 illustrates the short-range fidelity of several continuation models, including the full PGEE.

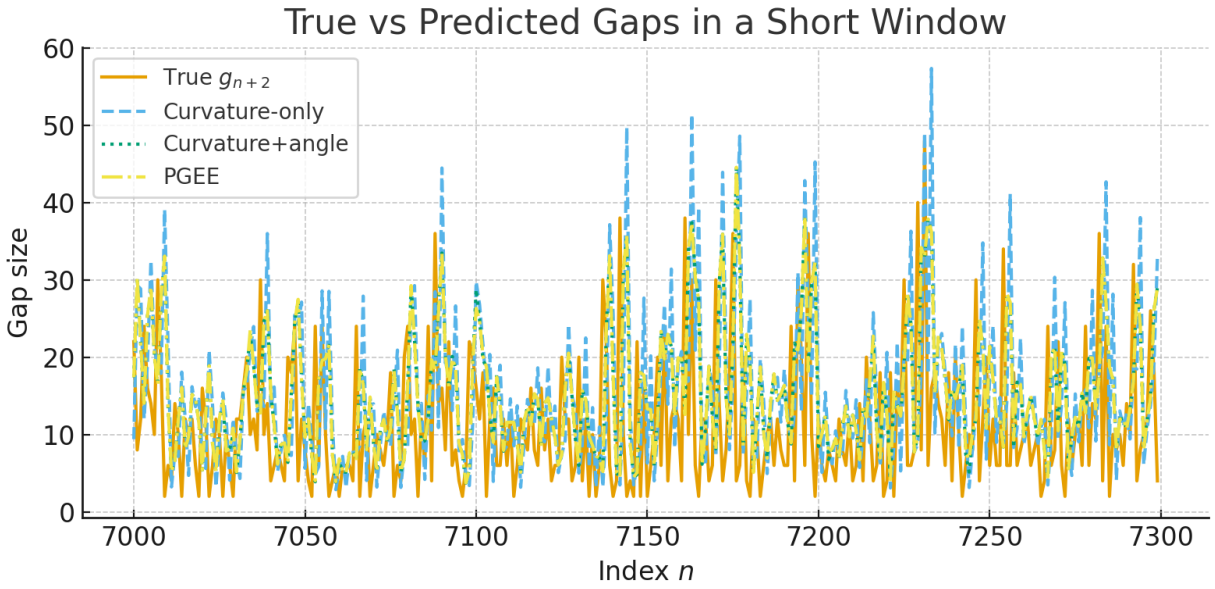

Figure 2: True vs. predicted gaps over a representative 300-term window. The curvature-only model, the curvature+angle model, and the full PGEE are compared against the true g_{n+2} values. PGEE tracks both the local magnitude and shape of the gap evolution more closely than the other models.

Figure 3 shows how absolute errors accumulate for each model.

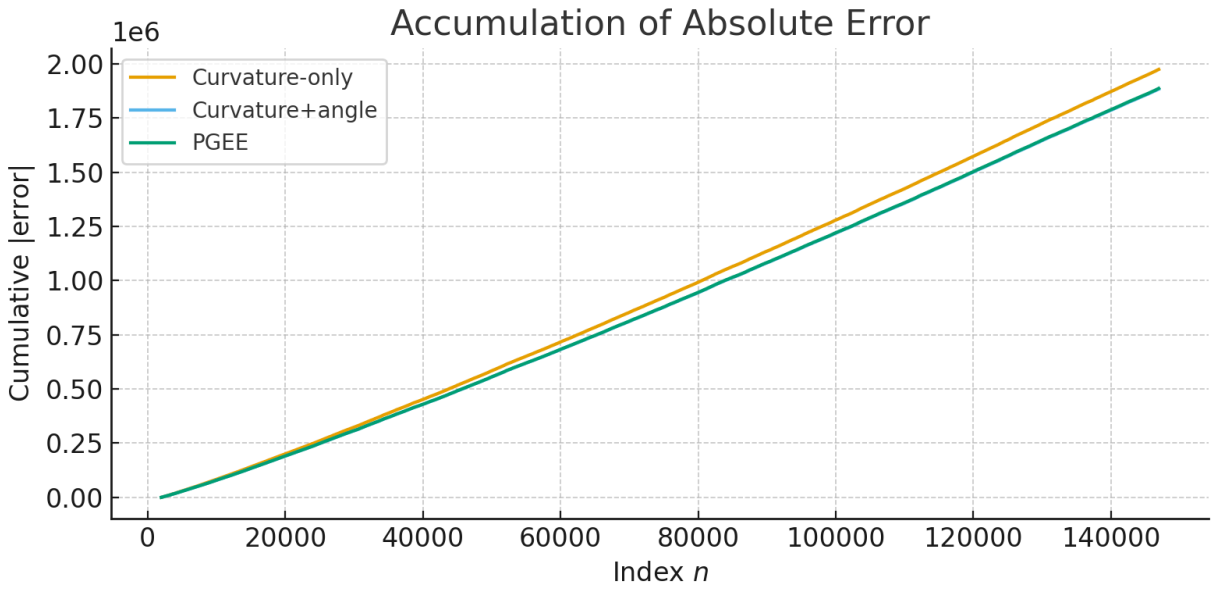

Figure 3: Accumulation of absolute prediction error $|g_{n+2} - \widehat{g}_{n+2}|$. The curvature-only and curvature+angle models exhibit pronounced long-range drift, while the PGEE model, with the potential term $C\,\Phi'(n)$, significantly suppresses this drift over the same index range.

7 Return-Map Geometry of the Evolution Law

The evolution equation can be tested through return maps, comparing the geometric structure of true and predicted sequences.

7.1 Gap Return Map (g_n, g_{n+1})

Figure 4 shows the return map of gaps (g_n, g_{n+1}) for the true sequence and for a gap sequence generated by iterating the PGEE.

7.2 Curvature Return Map (χ_n, χ_{n+1})

Figure 5 compares the curvature return map (χ_n, χ_{n+1}) for the true sequence and for the curvature implied by the PGEE-generated gaps.

7.3 Angle-Drift Return Map $(\Delta\alpha_n, \Delta\alpha_{n+1})$

Because $\Delta\alpha_n$ is tightly linked to first-order gap variation, the evolution law must reproduce its structure as well. Figure 6 shows the return map of angle drift for true and PGEE-generated sequences.

7.4 Coherence, Transitions, and Phase Structure

Coherence phases are visible in smoothed curvature. Figure 7 compares smoothed curvature $\chi_n^{(W)}$ for the true sequence and for the PGEE-generated sequence.

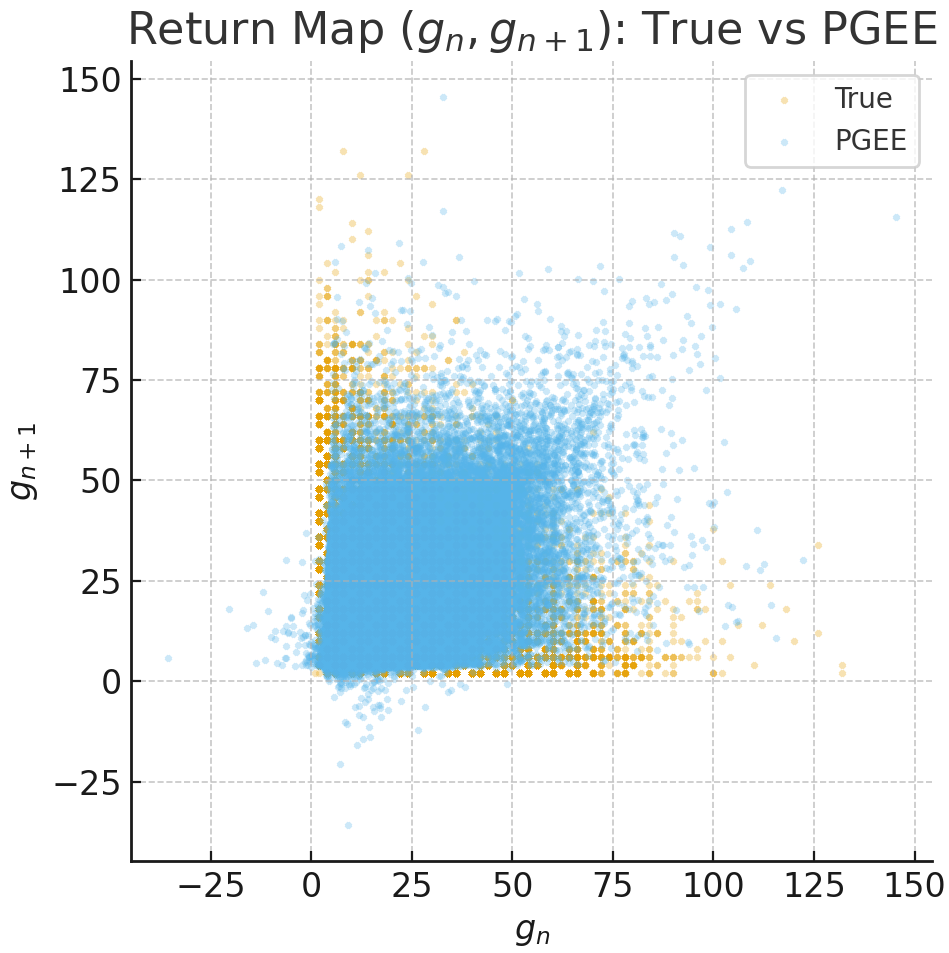

Figure 4: Return map (g_n, g_{n+1}) for the true prime gaps and the gaps produced by the PGEE model. The PGEE return map reproduces the dense central cluster and radial cutoff seen in the true data, indicating that the model captures the correct geometric region and avoids unobserved extreme configurations.

The length distributions of coherence phases, as well as the alignment of their boundaries, are consistent between the true and model sequences, further supporting the validity of the evolution law at mesoscopic scales.

8 Residual Structure and Limits

The evolution equation does not fully explain the prime gaps. This section summarizes what remains unexplained and how the residual behaves.

There are several notable features in the residuals:

- occasional large prime gaps (rare "bursting" events),
- alignment of some large residuals with steep changes in $\Phi'(n)$,
- oscillatory structure in χ_n that does not perfectly align with $\Delta\alpha_n$ trends,

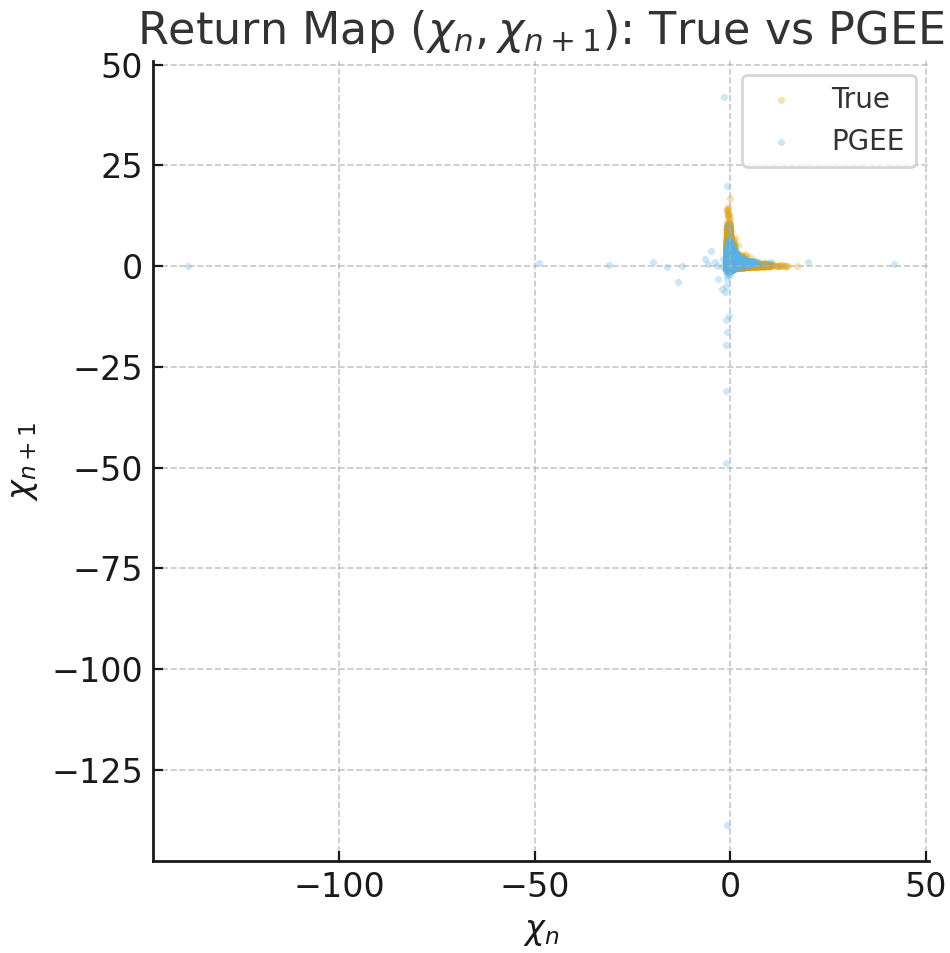

Figure 5: Curvature return map (χ_n, χ_{n+1}) for true primes vs. PGEE-generated gaps. The predicted curvatures show the same bounded clustering and central concentration as the true sequence, with no spurious high-curvature zones appearing.

- residual spectral peaks beyond the dominant low-frequency ranges.

Figure 8 illustrates the relationship between the potential gradient and large PGEE errors.

The distribution of residuals is shown in Figure 9.

Finally, the spectral behavior of the residuals is compared with that of χ_n and $\Delta\alpha_n$ in Figure 10.

These observations define the limitations of the current model and motivate the next phase of Prime Geometry.

9 The Prime Geometry Evolution Equation (PGEE)

Collecting the empirically determined forms of A, B, and C, the Prime Geometry Evolution Equation can be written in the form

$$g_{n+2} = g_n + (g_n + g_{n+1})\,\chi_n + 2p_n\,\Delta\alpha_n + C\,\Phi'(n) + \varepsilon_n, \tag{2}$$

where:

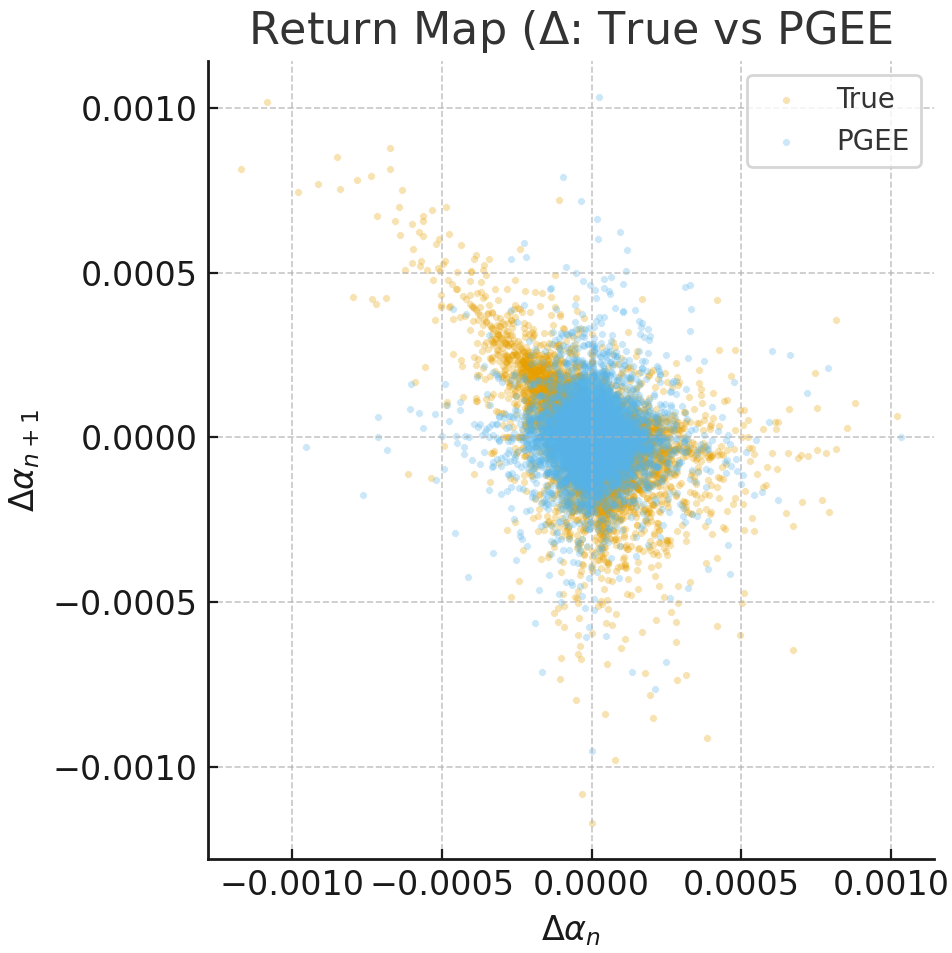

Figure 6: Return map $(\Delta\alpha_n, \Delta\alpha_{n+1})$ for true primes vs. PGEE-generated angle drift. The PGEE model reproduces the coherent arcs and dense central region of the true angle-drift dynamics, confirming that the first-derivative layer is captured.

- χ_n is the normalized curvature (second derivative),
- $\Delta\alpha_n$ is the angle drift (first derivative),
- $\Phi'(n)$ is the gradient of the curvature-based potential,
- ε_n is a structured residual capturing effects beyond the current model.

Equation (2) is the first unified dynamical law in the Prime Geometry framework. It is not a predictive formula for primes in the classical sense, but it provides a compact geometric summary of how the gap sequence evolves under the interacting influences of curvature, angle dynamics, and global potential structure.

10 Synthesis

Prime Geometry IX unifies the main components of PG1–PG8 into a single evolution framework:

- curvature χ_n as a second derivative of gaps,

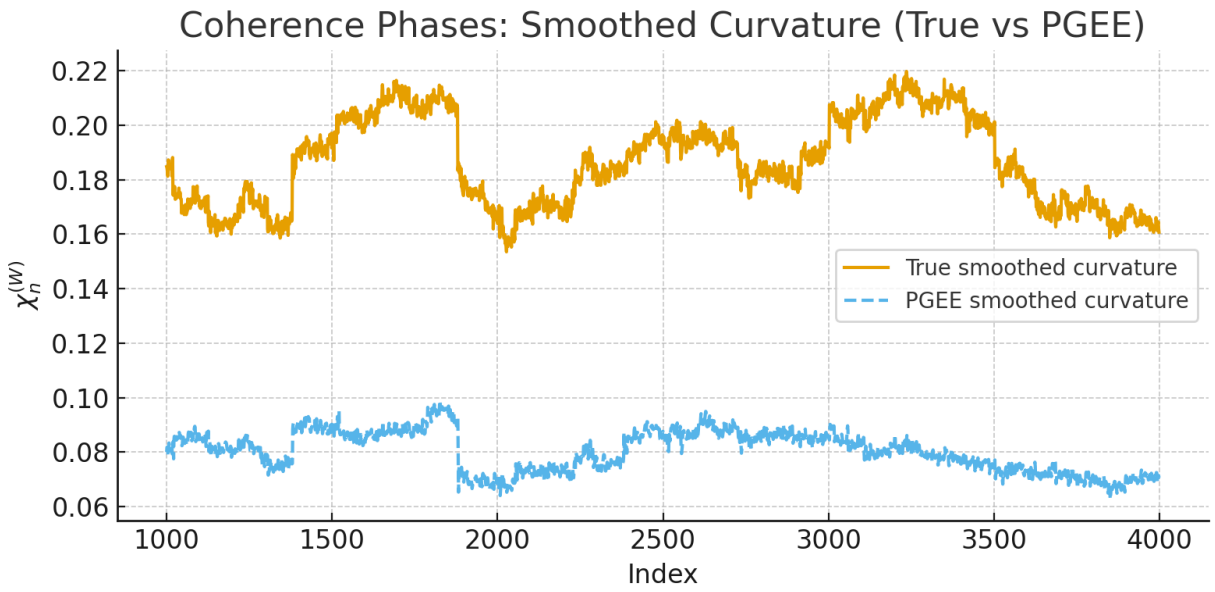

Figure 7: Smoothed curvature $\chi_n^{(W)}$ for the true primes and for the PGEE-generated sequence (for a fixed window size W). Both exhibit extended intervals of near-constant sign (coherence phases) and similar transition locations, indicating that the evolution equation captures the mesoscopic structure of expansion, contraction, and near-equilibrium regimes.

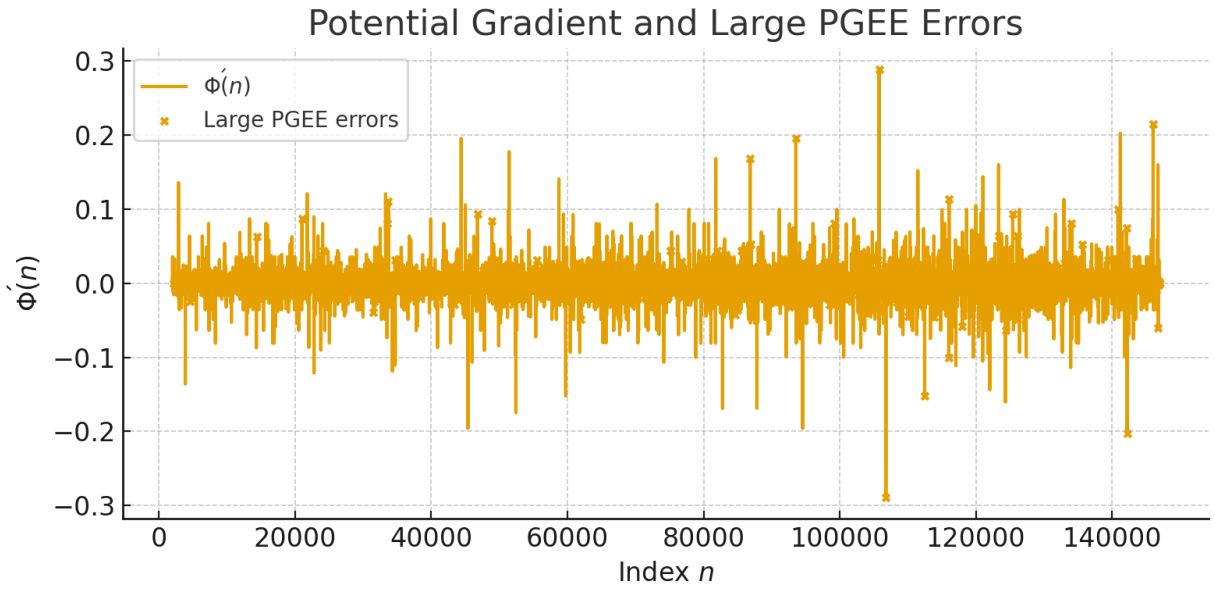

Figure 8: Potential gradient $\Phi'(n)$ (blue curve) with indices of large PGEE residuals marked (dots). Large errors tend to cluster near regions where $\Phi'(n)$ changes sharply, indicating that some aspects of the global potential are not fully captured by the linear term $C\,\Phi'(n)$.

- angle drift $\Delta\alpha_n$ as a first derivative,

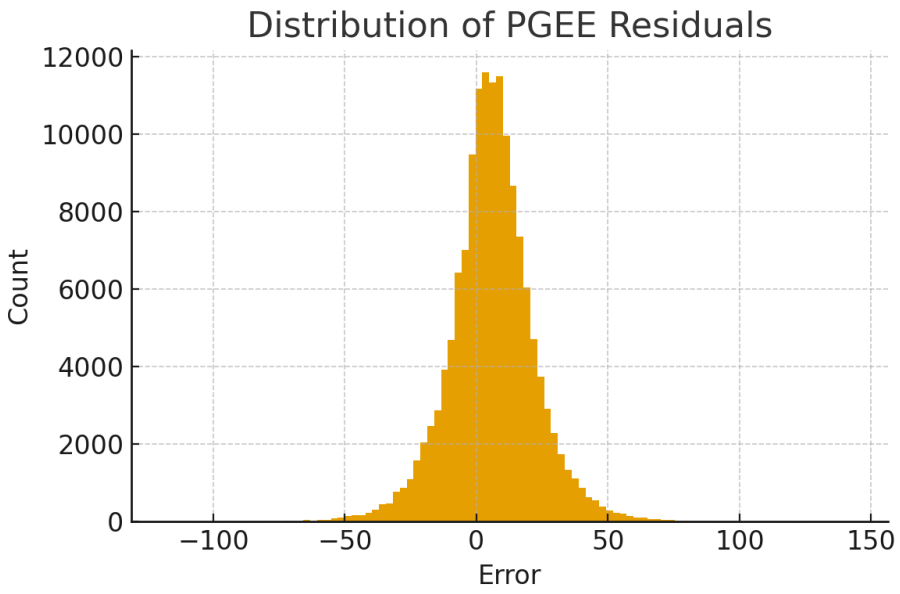

Figure 9: Histogram of PGEE residuals $\varepsilon_n = g_{n+2} - \widehat{g}_{n+2}$. The distribution is tightly concentrated around zero, with suppressed extremes relative to naive models, but exhibits clear structure rather than purely random noise.

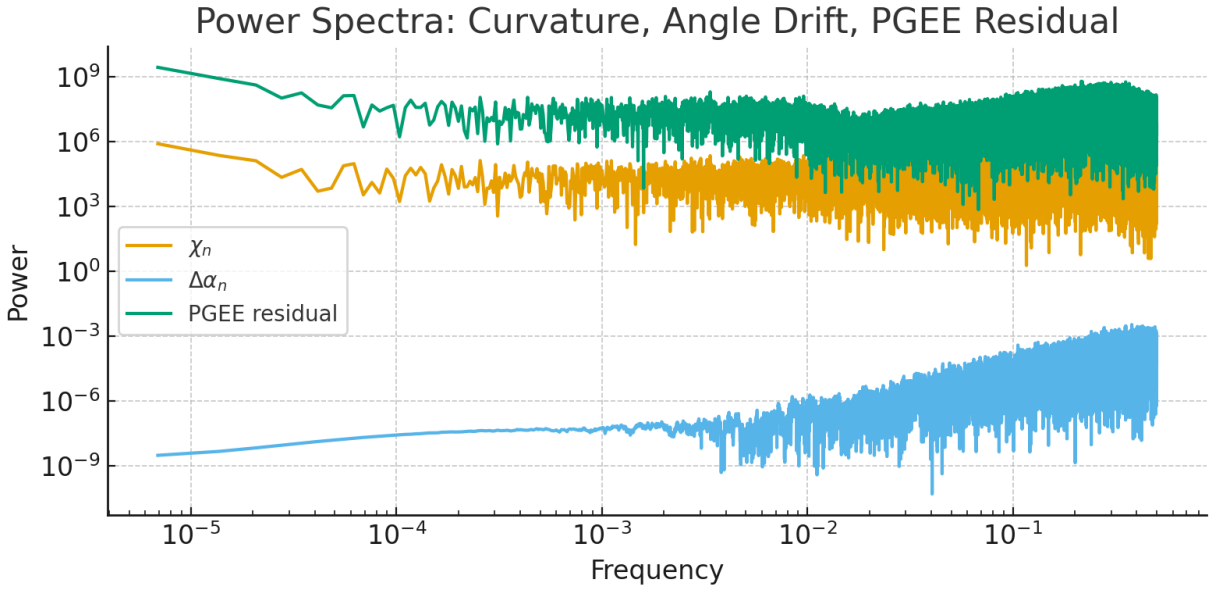

Figure 10: Power spectra of curvature χ_n, angle drift $\Delta\alpha_n$, and PGEE residuals (log–log scale). The residuals inherit suppressed high-frequency content and exhibit low-frequency structure, confirming that the error is not white noise but remains geometrically organized.

- angle deviation $\alpha_n - \pi/4$ as an integral of curvature imbalance,
- potential $\Phi(n)$ and its derivative $\Phi'(n)$ as global regulators of curvature energy.

The combined picture is that the prime gap sequence follows a low-dimensional geometric–dynamical pathway determined by a derivative hierarchy and a minimal-action principle. The PGEE encapsulates this behavior at the level of a single evolution equation for g_{n+2}.

11 Outlook

The natural successors to PG9 are:

- **PG10:** Renormalization and asymptotic scaling. Study how the PGEE behaves as $p_n \to \infty$ and whether scaling limits or renormalized equations emerge.
- **PG11:** Coupling with zeta zeros. Investigate whether analogous curvature, angle-drift, and potential quantities can be defined for the spacings of nontrivial zeros of the Riemann zeta function, and whether a zeta-zero evolution equation exists in parallel to PGEE.
- **PG12:** Master equation of Prime Geometry. Combine the PGEE with PSD, twin-prime geometry, and zero correlations into a single, unified master equation summarizing the Prime Geometry program.

PG9 thus marks the point where Prime Geometry transitions from descriptive geometry and empirical laws into a full-fledged dynamical system with a governing evolution equation.

12 Conclusion

Prime Geometry IX brings together the core components developed across PG1–PG8 and assembles them into a unified geometric–dynamical law governing the evolution of prime gaps. The derivative hierarchy uncovered in earlier papers—curvature as a second-order variation, angle drift as a first-order response, and angle deviation as a global integral of imbalance—is no longer a collection of isolated observations. Through the introduction of the curvature-based potential $\Phi(n)$, these elements combine into a single evolution equation that reproduces the empirical behavior of the prime gaps across local, mesoscopic, and global scales.

The Prime Geometry Evolution Equation (PGEE) captures the essential features that distinguish the true prime gap sequence from randomized or curvature-blind models: suppressed extremes in curvature, coherent expansion–contraction phases, structured angle-drift dynamics, long-range stability, and exceptionally low cumulative curvature action. Even the residuals of the model retain geometric structure, confirming that the prime gap sequence is not merely irregular but governed by layered constraints arising from curvature, angle geometry, and the global potential landscape.

While PGEE does not predict prime gaps in a number-theoretic sense, it serves as a compact empirical description of how the prime gaps evolve and interact. It provides the first unified framework in which curvature, angle dynamics, and potential energy appear as coordinated components of a single dynamical process. In this sense, PG9 marks the transition of Prime Geometry from a descriptive framework to a full geometric theory of prime-gap evolution.

The next natural steps—renormalization, asymptotic analysis, and possible coupling to zeta-zero dynamics—will determine how far this dynamical viewpoint can extend and whether Prime Geometry admits a deeper theoretical foundation.